LETTERS

A trehalose metabolic enzyme controls inflorescence architecture in maize

Namiko Satoh-Nagasawa[1], Nobuhiro Nagasawa[2], Simon Malcomber[3]†, Hajime Sakai[2] & David Jackson[1]

Inflorescence branching is a major yield trait in crop plants controlled by the developmental fate of axillary shoot meristems[1]. Variations in branching patterns lead to diversity in flower-bearing architectures (inflorescences) and affect crop yield by influencing seed number or harvesting ability[2,3]. Several growth regulators such as auxins, cytokinins and carotenoid derivatives regulate branching architectures[4]. Inflorescence branching in maize is regulated by three *RAMOSA* genes[5]. Here we show that one of these genes, *RAMOSA3* (*RA3*), encodes a trehalose-6-phosphate phosphatase expressed in discrete domains subtending axillary inflorescence meristems. Genetic and molecular data indicate that *RA3* functions through the predicted transcriptional regulator *RAMOSA1* (*RA1*)[5]. We propose that *RA3* regulates inflorescence branching by modification of a sugar signal that moves into axillary meristems. Alternatively, the fact that *RA3* acts upstream of *RA1* supports a hypothesis that RA3 itself may have a transcriptional regulatory function.

Trehalose is a disaccharide composed of two glucose units. It is present in all kingdoms and has functions in carbohydrate storage, stress protection and metabolic regulation[6,7]. Until fairly recently it was thought to be present in only a small number of desiccation-tolerant plants (reviewed in ref. 8) because endogenous trehalose levels are very low in most plants. However, trehalose biosynthesis genes are present in all plants, and recent data indicate that this sugar functions in stress protection as well as in carbohydrate utilization and growth[9–11]. Trehalose biosynthesis occurs in two steps[8]. First, trehalose 6-phosphate (T6P) is made from UDP-glucose and glucose 6-phosphate by T6P synthase (TPS), and T6P is then converted to trehalose by T6P phosphatase (TPP)[12]. Here we show that *RAMOSA3* controls maize inflorescence architecture and encodes a functional TPP enzyme, implying a previously unrecognized role for trehalose metabolism in developmental signalling and morphogenesis. Although trehalose biosynthetic enzymes are ubiquitous, this is conclusive evidence that they have a defined developmental function. Our findings greatly extend previous studies that suggested such a function but did not identify any specific developmental process or stage that is affected by such enzymes. For example, heterologous expression of bacterial trehalose enzymes can perturb development[11,13]. Furthermore, *tps1* mutants in *Arabidopsis* are embryo lethal[10], and *TPS1* is required for sustained growth in *Arabidopsis*, including during the floral transition[14].

ramosa3 (*ra3*) is a classical mutant of maize[15]. Maize has two types of flower-bearing structure with different architectures that were selected during maize domestication to enhance its utility as an agricultural crop[5]. The terminal male inflorescence, or tassel, has long branches at its base and a central spike that bears shorter branches containing spikelet pairs (Fig. 1c). In contrast, the female inflorescences, or ears, are positioned laterally and contain only short branches, a trait that is thought to aid in the efficient packing and harvesting of seeds (Fig. 1a). *RA3* is required for this specialized architecture, because *ra3* mutant tassels have additional long branches (Fig. 1d; wild-type (B73) 7.9 ± 0.2 (mean ± s.e.m.); *ra3* 15.4 ± 0.8 branches) and *ra3* mutant ears have abnormal long branches at their bases (Fig. 1b). A detailed analysis of ear development by scanning electron microscopy (SEM) showed that there was no morphological difference between wild-type and *ra3* inflorescences

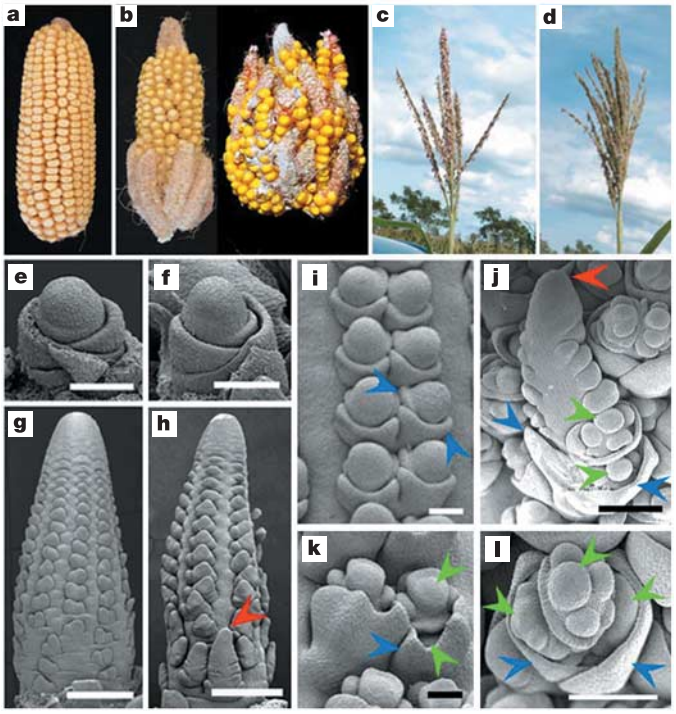

Figure 1 | *ra3* mutant phenotypes. **a**, Mature wild-type ear. **b**, Mature *ra3* ears introgressed into B73 (left) or in a mixed genetic background (right) had abnormal branches and irregular seed rows. **c**, Mature wild-type tassel. **d**, Mature *ra3* tassel with additional long branches. **e–l**, SEM of wild-type ear development (**e**, **g**, **i**, **k**) and *ra3* ear development (**f**, **h**, **j**, **l**): before initiation of axillary meristems (**e**, **f**), ears 2 mm long (**g**, **h**), ears 5 mm long (**i**, **j**) and ears 1 cm long (**k**, **l**). In the *ra3* mutant (**h**) some SPMs changed their identity and formed indeterminate branches, resembling the long branches at the base of the tassel (red arrowhead). SMs in the wild type (**i**, **k**) produced a pair of FMs (green arrowheads) subtended by glumes (blue arrowheads), but in *ra3* (**j**) after the production of FMs they sometimes converted to indeterminate branches. In other cases, SMs in *ra3* (**l**) made multiple FMs. Scale bars, 100 μm (**e**, **f**, **i**, **j**), 500 μm (**g**, **h**) and 200 μm (**k**, **l**).

[1]Cold Spring Harbor Laboratory, 1 Bungtown Road, Cold Spring Harbor, New York 11724, USA. [2]DuPont Crop Genetics Experimental Station E353, Wilmington, Delaware 19880, USA. [3]Department of Biology, University of Missouri-St Louis, St Louis, Missouri 63121, USA. †Present address: Department of Biological Sciences, California State University–Long Beach, Long Beach, California 90840, USA.

before axillary inflorescence meristems were produced (Fig. 1e, f). However, once axillary meristems were initiated in *ra3* mutants, they showed a general loss of determinacy as well as changes in identity (Fig. 1h, j, l). In normal ears, the inflorescence meristem initiates axillary meristems (spikelet pair meristems (SPMs); Fig. 1g), which are determinate structures producing two spikelet meristems (SMs; Fig. 1i). Each SM in turn produces two floral meristems[3] (FMs; Fig. 1k). In *ra3* mutants the axillary meristems were enlarged and acquired abnormal identity (Fig. 1h, j) or became indeterminate (Fig. 1l), leading to the production of long branches (Fig. 1h, j) or more FMs (Fig. 1l). Similar developmental defects were observed in the tassel, although at a lower frequency (not shown). We therefore conclude that *RA3* acts to establish the correct identity and determinacy of axillary meristems in both male and female inflorescences.

With the use of bulked segregant analysis[16] *RA3* was mapped to chromosome 7, and by fine mapping it was located to a single bacterial artificial chromosome (BAC), which was sequenced. This sequence was used to design further markers that delimited the *RA3* locus to a single predicted open reading frame (ORF) (Supplementary Fig. 1a, b and Supplementary Table 1). Identification of lesions in seven *ra3* alleles all mapping to the same ORF confirmed unambiguously that this encodes *RA3* (Supplementary Table 2). *RA3* encodes a predicted protein of 361 amino-acid residues with significant similarity to TPPs[9]. A non-conserved amino-terminal region of about 80 residues is followed by the TPP domain, which contains two conserved 'phosphatase boxes'[8,17] (Supplementary Fig. 1b). Most of the *ra3* mutant alleles encode frame shifts leading to a stop codon before the second phosphatase box and to a strong mutant phenotype. One of them, *ra3-fea1*, has no detectable transcript in immature ears (Supplementary Fig. 1c). They are therefore likely to be null alleles. The *ra3-NI* allele has a milder phenotype (not shown) and has a premature stop after the second phosphatase box (Supplementary Table 2).

About 10 kilobases upstream of *RA3*, a highly similar gene was discovered and dubbed *SISTER OF RA3* (*SRA*) (Supplementary Fig. 1a). The conserved syntenic region of rice contained only a single TPP gene, gi33146623. *RA3*, *SRA* and gi33146623 share about 70% amino-acid identity within the TPP domain, and about 65% identity overall. We searched for closely related homologues in GenBank and in the maize genome sequence assemblies[18–20] and amplified *RA3*/*SRA*-like genes from a range of other grasses. A phylogenetic analysis of TPP genes was conducted with bayesian methods[21] (Supplementary Fig. 2). This phylogenetic analysis estimates a well-supported RA3/SRA clade (100% clade credibility [CC]) nested within a well-supported clade (97% CC) of grass TPP genes. Although the exact placement of the *RA3*/*SRA* duplication event is still in question, our best estimate is that it occurred near the base of the major diversification of the grasses. Because of multiple duplication events within or before the origin of the grasses, the closest *Arabidopsis* TPP genes (*TPPB* (ref. 22) and At1g22210) cannot be considered orthologous to either *RA3* or *SRA*.

RA3 was expressed predominantly in young inflorescences, at the stage where axillary meristem primordia were being initiated. In contrast, *SRA* was expressed more widely in all organs tested and showed the highest expression in roots (Fig. 2a). *In situ* hybridization revealed a localized pattern of *RA3* expression in cup-shaped domains at the base of axillary meristems in young ear primordia, and in a stripe between upper and lower florets (Fig. 2b–f). This expression was specific for *RA3*, because it was not seen in *ra3-fea1* mutant ears (Fig. 2g). In the tassel, *RA3* was not expressed as the long branches were initiated (not shown) but was expressed at the base of SPMs (Fig. 2h). These patterns are consistent with a function of *RA3* in promoting determinacy of axillary meristems in the tassel. Together with the developmental analysis, the restricted expression pattern suggests a highly specific developmental role for *RA3* in inflorescence development. *In situ* hybridization with an *SRA*-specific probe in maize inflorescences failed to detect a localized expression pattern, indicating that it might be expressed at a low level in all or many cells (not shown).

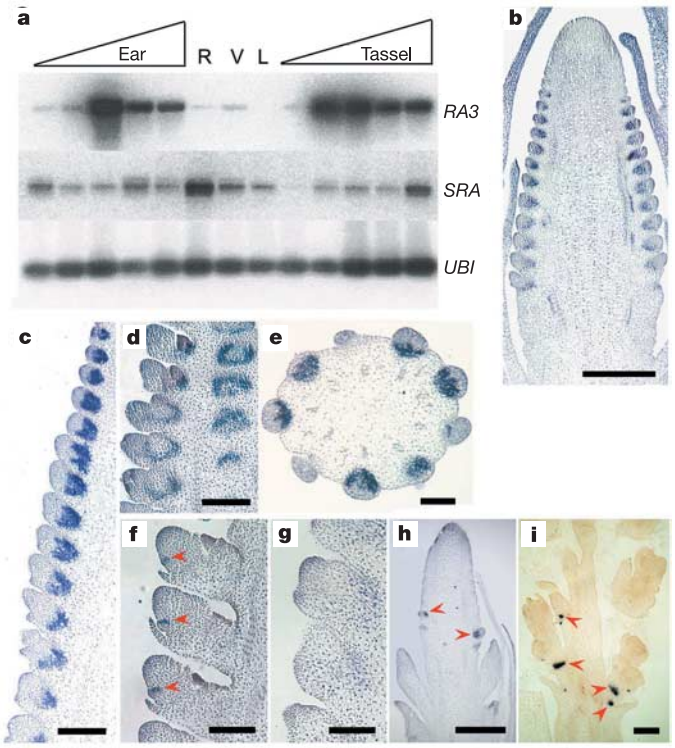

Figure 2 | Developmental expression of *RA3* and *SRA*. **a**, RT–PCR of mRNAs from root (R), vegetative apex (V), young leaves (L) and ear or tassel inflorescence primordia. The triangles represent increasing inflorescence size, from the stage before axillary meristem initiation to ears and tassels about 1.5 cm long. **b–f**, Detection of *RA3* expression by *in situ* hybridization. **b**, Longitudinal section of an ear 2 mm long. **c**, **d**, Longitudinal median and glancing sections of ears 7 mm long. **e**, Transverse section of ear 7 mm long. **f**, Longitudinal section of developing spikelets. **g**, Control section showing lack of hybridization signal in a *ra3-fea1* ear. **h**, Longitudinal section of a tassel 2 mm long. **i**, *In situ* hybridization of the rice *SRA* gene in a longitudinal section of a rice inflorescence. Red arrowheads show the expression domain of *RA3* (**f**, **h**) and rice *SRA* (**i**). Scale bars, 500 μm (**b**, **h**), 200 μm (**c**, **d**, **e**) and 100 μm (**f**, **g**, **i**).

To investigate whether *RA3*-like genes might also have a developmental function in other plants, we isolated a *RA3* orthologue from sorghum and examined its expression pattern. This gene was expressed in a similar localized manner to that of *RA3* (not shown), suggesting that *RA3* function is conserved in other grasses. We also examined expression of the closest rice homologue, which was phylogenetically most similar to *SRA* (Supplementary Fig. 2). It was expressed widely, with higher expression levels in both root and young inflorescence (Supplementary Fig. 3). However, like *RA3* it showed a localized expression domain at the base of axillary inflorescence branches and beneath the spikelets (Fig. 2i), indicating that this gene might also regulate inflorescence development in rice.

We next examined whether RA3 had TPP activity, a possibility indicated by its sequence similarity. RA3 TPP activity was tested by a phosphate release assay with the use of recombinant RA3 protein[23]. RA3 catalysed phosphate release from T6P but not from other sugar phosphates or a general substrate of protein phosphatases, indicating that it might act specifically as a TPP (Supplementary Fig. 4a). TPP activity was also confirmed by complementation of a yeast TPP mutant[24] by RA3 (Supplementary Fig. 4b). Our data therefore indicate that RA3 acts specifically as a TPP *in vivo*.

A *RAMOSA* pathway in maize was recently proposed in which *RAMOSA2* (*RA2*) acts upstream of *RA1* (ref. 5). To determine

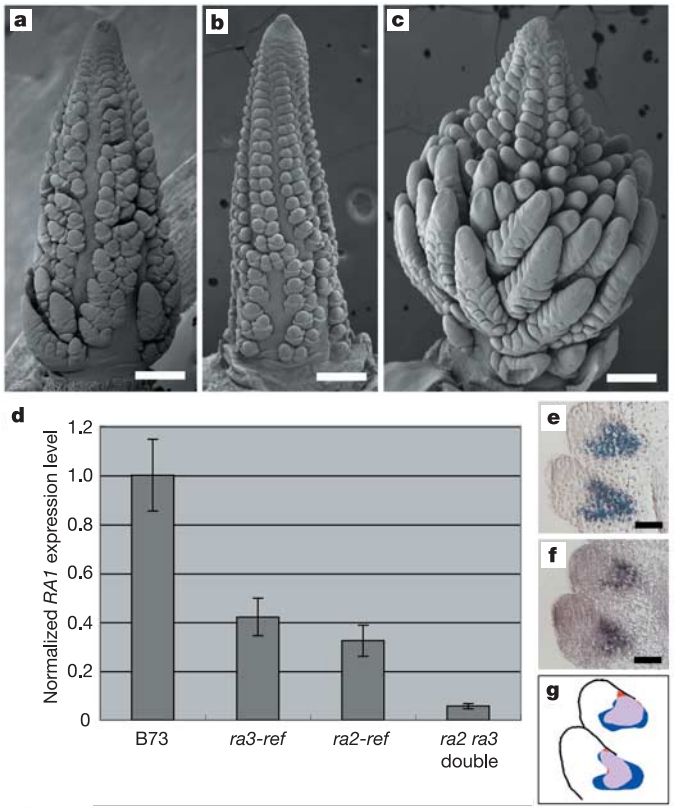

Figure 3 | *ra3* enhances a weak *ra1* mutant, and *RA1* expression is reduced in *ra3* mutants. a, An *ra3* mutant ear had abnormally long branches restricted to the base of the ear. **b**, The weak *ra1-RS* allele had ears with no abnormal long branches, but occasional disruption of spikelet rows. Red arrowheads show the irregular rows. **c**, A *ra3; ra1-RS* double mutant showed a strongly enhanced phenotype, with all axillary meristems growing out as long branches. Scale bars, 500 μm. **d**, *RA1* expression was reduced in *ra2*, *ra3* and in *ra2 ra3* double mutants. Each data point is an average of three independent RT–PCR assays, and error bars indicate s.e.m. **e–g**, *RA3* (**e**) and *RA1* (**f**) are expressed in highly overlapping domains (**g**; RA3 in blue, *RA1* in red, overlapping domain in pink). Scale bars, 50 μm.

whether *RA3* also acts in this genetic pathway, we first examined *RA3* expression in *ra1* and *ra2* mutants. No significant change in the level or localization of *RA3* expression in these mutants was observed (data not shown). We next made double mutants between *ra3-ref* (Fig. 3a) and *ra1-RS*, a weak allele of *ra1* (ref. 5) (Fig. 3b). In ears (Fig. 3c) and tassels (not shown), the double mutants showed a strongly enhanced branching phenotype that resembled a strong *ra1* allele[5]. Expression levels of *RA1* in *ra2* mutants, in *ra3* mutants and in *ra2 ra3* double mutants in the ears were also studied. As previously reported, *RA1* expression was lower in *ra2* mutants[5]. *RA1* expression was also lower in *ra3* mutants and even lower in *ra2 ra3* double mutants (Fig. 3d), which had a similar phenotype to a strong *ra1* allele (not shown). Our data indicate that *RA3*, like *RA2*, acts upstream of *RA1* to regulate meristem identity and determinacy in maize inflorescences. Consistent with this hypothesis is the observation that *RA3* and *RA1* are expressed in overlapping domains in the developing ear (Fig. 3e–g). The sorghum *RA1* (ref. 5) and *RA3* genes are expressed similarly to maize *RA1* (ref. 5) and *RA3*, suggesting at least partial conservation of the *RAMOSA* pathway in the grasses. However, if the rice *SRA* gene also regulates inflorescence development, it must act through genes other than *RA1*, which is absent from this species[5].

Our results indicate that trehalose metabolism can regulate a specific developmental pathway. The low endogenous levels of trehalose in most plants and the existence of multiple copies of trehalose biosynthetic genes has led to speculation that there are spatially restricted regulatory roles for these genes[9]. Our data are also consistent with observations that the modulation of endogenous and exogenous trehalose levels affects plant growth[13,14]. However, trehalose may act as a signal in a specific developmental pathway, because we showed that a functional TPP enzyme acts upstream of the *RA1* transcription factor to regulate inflorescence branching. The effect of *RA3* on inflorescence architecture could be mediated directly through the modulation of trehalose or T6P levels. Currently the only known targets of these sugars in plants function in metabolic signalling, in which T6P seems to be the important signal[11,13,25,26]. The highly localized expression pattern of *RA3* and the presence of multiple TPP genes in plants mean that it may be impossible to measure differences in trehalose and T6P levels in *ra3* mutants accurately, because it is not feasible to measure these metabolites *in situ*. Indeed, our efforts so far have not succeeded in detecting reproducible differences in levels of these sugars in whole inflorescence extracts of *ra3* mutants (N.S.-N., D.J. and M. Paul, unpublished observations).

RA3 is expressed in localized domains of cells subtending, but not within, the axillary meristems in the inflorescence, indicating that it acts non-cell-autonomously. We speculate that if *RA3* does indeed act through the modulation of trehalose or T6P levels, these sugars may act as a mobile short-range signal, to regulate meristem identity and determinacy. Alternatively, our demonstration that *RA3* acts upstream of the *RA1* transcription factor would be consistent with a role for RA3 itself in transcriptional regulation, similar to that described for some glycolytic enzymes (reviewed in ref. 27). It will be interesting to investigate further the molecular mechanism of *RA3* function, and the role of other *RA3*-like genes, to determine whether they contributed to the evolution of the unique maize inflorescence architecture that makes it one of our most successful crops[2,5].

METHODS

Plant materials. Plants were grown in the greenhouse or in the field, under standard conditions. The wild-type line used was B73. Inflorescences were dissected and fixed for *in situ* hybridization or imaged by SEM as described[28].

Mapping. Both the original *ra3-ref* allele and the *ra3-fea1* allele that we isolated from a *Mutator* transposon line were used to construct mapping populations with the wild-type line B73. Approximately 1,000 mutant individuals were used for fine mapping with molecular markers from BAC end sequences, overgoes (og; Supplementary Fig. 1) and non-repetitive sequences ('cold bands' (cb); Supplementary Fig. 1). 'Cold bands' were identified as DNA fragments on Southern blots of BAC clones that hybridized strongly to the same BAC probe but not to maize genomic DNA.

Molecular biology. Standard protocols were used for maize DNA isolation, Southern blotting and *in situ* hybridization[28]. For labelling of *RA3* and *RA1* (ref. 5) on adjacent sections, both probes were hybridized and detected with the standard substrate[28] and the images were scanned into Adobe Photoshop before false colouring and superimposition. For analysis by polymerase chain reaction with reverse transcription (RT–PCR) in Supplementary Fig. 1c and Fig. 2a, poly(A)$^+$ RNA was isolated with an Oligotex mRNA mini kit (Qiagen) in accordance with the manufacturer's protocol. The primers NS432 (5′-TCGTGAC AAGCATCGCAAGCA-3′) and NS411 (5′-GCGCATCAGCTAGGTTGTTGT-3′), og15UTR (5′-ATCCATTCATCCGTGTGGTGT-3′) and og13UTR (5′-CCTGC TGACTGGACCATGACTA-3′) were used to amplify *RA3* and *SRA* transcripts, respectively, with the one-step RT–PCR kit (Qiagen). The control primers Ubi 5′ (5′-TAAGCTGCCGATGTGCCTGCGTCG-3′) and Ubi 3′ (5′-CTGAAAGAC AGAACATAATGAGCACAG-3′) were used to amplify *UBIQUITIN* (*UBI*) transcripts. PCR conditions were 94 °C for 30 s, 55 °C for 30 s and 72 °C for 90 s (20 cycles). The PCR cycle number was limited to ensure semiquantitative amplification, and no PCR product was visible on ethidium-bromide-stained agarose gels. The gels were Southern blotted and probed with a *RA3*, *SRA* or *UBI* probe. For RT–PCR analysis in Fig. 3d, total RNA was isolated from ears that had initiated only SPMs and semiquantitative RT–PCR was performed as described[5]. The relative *RA1* expression levels measured by RT–PCR were normalized against a ubiquitin control.

Received 16 February; accepted 15 March 2006.

1. Ward, S. P. & Leyser, O. Shoot branching. *Curr. Opin. Plant Biol.* **7**, 73–78 (2004).

2. Doebley, J. Mapping the genes that made maize. *Trends Genet.* **8,** 302–307 (1992).
3. Bommert, P., Satoh-Nagasawa, N., Jackson, D. & Hirano, H. Genetics and evolution of inflorescence and flower development in grasses. *Plant Cell Physiol.* **46,** 69–78 (2005).
4. Schmitz, G. & Theres, K. Shoot and inflorescence branching. *Curr. Opin. Plant Biol.* **8,** 506–511 (2005).
5. Vollbrecht, E., Springer, P. S., Goh, L., Buckler, E. S. & Martienssen, R. Architecture of floral branch systems in maize and related grasses. *Nature* **436,** 1119–1126 (2005).
6. Strom, A. R. & Kaasen, I. Trehalose metabolism in *Escherichia coli*: stress protection and stress regulation of gene expression. *Mol. Microbiol.* **8,** 205–210 (1993).
7. Thevelein, J. M. & Hohmann, S. Trehalose synthase: guard to the gate of glycolysis in yeast? *Trends Biochem. Sci.* **20,** 3–10 (1995).
8. Goddijn, O. J. & van Dun, K. Trehalose metabolism in plants. *Trends Plant Sci.* **4,** 315–319 (1999).
9. Leyman, B., Van Dijck, P. & Thevelein, J. M. An unexpected plethora of trehalose biosynthesis genes in *Arabidopsis thaliana*. *Trends Plant Sci.* **6,** 510–513 (2001).
10. Eastmond, P. J., Li, Y. & Graham, I. A. Is trehalose-6-phosphate a regulator of sugar metabolism in plants? *J. Exp. Bot.* **54,** 533–537 (2003).
11. Schluepmann, H., Pellny, T., van Dijken, A., Smeekens, S. & Paul, M. Trehalose 6-phosphate is indispensable for carbohydrate utilization and growth in *Arabidopsis thaliana*. *Proc. Natl Acad. Sci. USA* **100,** 6849–6854 (2003).
12. Cabib, E. & Leloir, L. F. The biosynthesis of trehalose phosphate. *J. Biol. Chem.* **231,** 259–275 (1958).
13. Schluepmann, H. *et al.* Trehalose mediated growth inhibition of *Arabidopsis* seedlings is due to trehalose-6-phosphate accumulation. *Plant Physiol.* **135,** 879–890 (2004).
14. van Dijken, A. J., Schluepmann, H. & Smeekens, S. C. *Arabidopsis trehalose-6-phosphate synthase 1* is essential for normal vegetative growth and transition to flowering. *Plant Physiol.* **135,** 969–977 (2004).
15. Perry, H. S. Maize Genetics/Genomics Database [online] ⟨http://www.maizegdb.org/⟩.
16. Michelmore, R. W., Paran, I. & Kesseli, R. V. Identification of markers linked to disease-resistance genes by bulked segregant analysis: A rapid method to detect markers in specific genomic regions by using segregating populations. *Proc. Natl Acad. Sci. USA* **88,** 9828–9832 (1991).
17. Thaller, M. C., Schippa, S. & Rossolini, G. M. Conserved sequence motifs among bacterial, eukaryotic, and archaeal phosphatases that define a new phosphohydrolase superfamily. *Protein Sci.* **7,** 1647–1652 (1998).
18. Plant Genome DataBase. [online] ⟨http://www.plantgdb.org/prj/GSSAssembly/⟩.
19. The Institute for Genomic Research. The TIGR Maize Database [online] ⟨http://www.tigr.org/tdb/tgi/maize/⟩.
20. Emrich, S. J. *et al.* A strategy for assembling the maize (*Zea mays* L.) genome. *Bioinformatics* **20,** 140–147 (2004).
21. Huelsenbeck, J. P. & Ronquist, F. MrBayes: Bayesian inference of phylogenetic trees. *Bioinformatics* **17,** 754–755 (2001).
22. Vogel, G., Aeschbacher, R. A., Muller, J., Boller, T. & Wiemken, A. Trehalose-6-phosphate phosphatases from *Arabidopsis thaliana*: identification by functional complementation of the yeast *tps2* mutant. *Plant J.* **13,** 673–683 (1998).
23. Klutts, S. *et al.* Purification, cloning, expression, and properties of mycobacterial trehalose-phosphate phosphatase. *J. Biol. Chem.* **278,** 2093–2100 (2003).
24. De Virgilio, C. *et al.* Disruption of *TPS2*, the gene encoding the 100-kDa subunit of the trehalose-6-phosphate synthase/phosphatase complex in *Saccharomyces cerevisiae*, causes accumulation of trehalose-6-phosphate and loss of trehalose-6-phosphate phosphatase activity. *Eur. J. Biochem.* **212,** 315–323 (1993).
25. Pellny, T. K. *et al.* Genetic modification of photosynthesis with *E. coli* genes for trehalose synthesis. *Plant Biotechnol. J.* **2,** 71–82 (2004).
26. Kolbe, A. *et al.* Trehalose-6-phosphate regulates starch synthesis via posttranscriptional redox activation of ADP-glucose pyrophosphorylase. *Proc. Natl Acad. Sci. USA* **102,** 11118–11123 (2005).
27. Kim, J.-w. & Dang, C. V. Multifaceted roles of glycolytic enzymes. *Trends Biochem. Sci.* **30,** 142–150 (2005).
28. Taguchi-Shiobara, F., Yuan, Z., Hake, S. & Jackson, D. The *fasciated ear2* gene encodes a leucine rich repeat receptor like protein that regulates shoot meristem proliferation in maize. *Genes Dev.* **15,** 2755–2766 (2001).

Supplementary Information is linked to the online version of the paper at www.nature.com/nature.

Acknowledgements We thank C. Carson and E. Coe for initial molecular mapping of *RA3*; S. Hake for the *fea1-Mu* line; N. Inada, E. Irish, J. Linder and E. Vollbrecht for *ra3* alleles; T. Mulligan for plant care; J. Andersen, N. Kobayashi-Simorowski and N. Tonks for help with phosphatase assays; V. Koroth Edavana for suggestions about the *Mycobacterium* TPP clone; P. Dahl, D. Goto, K. Noma and T. Phelps-Durr for suggestions for the yeast complementation test; J. Kossuth for help with DNA sequencing; and E. Kellogg, W. Lukowitz, J. Simorowski, E. Vollbrecht, and members of the Jackson laboratory for comments on the manuscript. Funding was provided by the National Science Foundation, Plant Genome Research Program, and the National Research Initiative of the USDA Cooperative State Research, Education and Extension Service (to D.J.).

Author Contributions N.S.-N. performed the SEM analyses, *RA3* mapping, RT–PCRs, *in situ* hybridizations, double-mutant analyses, phosphatase assay and yeast complementation test. N.N. helped with *RA3* mapping and provided the material for RT–PCR in rice. S.M. performed phylogenetic analyses and *in situ* hybridizations in rice. H.S. organized the collaboration. D.J. supervised the research and wrote the paper. All authors discussed the results and commented on the manuscript.

Author Information Accession numbers for gene sequences are listed in Supplementary Fig. 2. Reprints and permissions information is available at npg.nature.com/reprintsandpermissions. The authors declare no competing financial interests. Correspondence and requests for materials should be addressed to D.J. (jacksond@cshl.edu).